Nonanalyticities of thermodynamic functions in finite noninteracting Bose gases within an exact microcanonical ensemble

Hui-yi Tang and Yong-li Ma*

State Key Laboratory of Surface Physics and Department of Physics, Fudan University, Shanghai 200433, China

(Received 26 January 2011; published 23 June 2011)

Within an exact microcanonical (MC) ensemble, we study the nonanalyticities of thermodynamic functions research in finite noninteracting Bose gases in traps. The results show that there exists a rich oscillatory behavior of MC thermodynamical quantities as a function of a system's total energy E (e.g., nonmonotonous temperature, nonanalytic and negative specific heats, and microscopic phase transitions). The origin of these nonanalyticities comes directly from the inverted curvature entropy $S(E)$ with respect to E and the behaviors are different in different trap geometries, boundary conditions, and energy spectrum configurations. Contrary to the usual grandcanonical and canonical results, there exists Bose condensation and the nonanalyticities in the two-dimensional finite noninteracting Bose systems with different traps. We also discuss the critical temperature dependence on the particle number N with different ensembles, traps, and boundary conditions. In large enough N, almost all the results of the thermodynamical quantities become smooth, which are similar to the usual canonical behaviors. We emphasize the finite-size effects on the MC entropy change, which should, in principle, be observable in suitably designed experiments of the small systems.

DOI: 10.1103/PhysRevE.83.061135 PACS number(s): 05.30.Ch, 64.70.Tg, 03.75.Hh, 67.10.Fj

I. INTRODUCTION

Phase transition as a natural phenomena has been studied thoroughly during the past century. Its characteristics are usually associated with the nonanalyticity of the thermodynamic functions in grandcanonical and canonical ensembles, but occurs in the thermodynamic limit only corresponding to the infinite value of particle number N, system volume V, and total energy E with the particle number density N/V and energy per particle E/N remain constant. During the past decades the rapid experimental progress led to an increasing interest in the studying of thermodynamic properties of small systems [e.g., sodium clusters [1,2], two-dimensional (2D) Coulomb clusters in dusty plasmas [3,4], cluster fission [5], Bose-Einstein condensation (BEC) in magnetooptical traps [6], and so on]. But the canonical and grandcanonical frameworks are inadequate as the basis to understanding the phenomena in these small systems. Thus we turn to the microcanonical (MC) ensemble which is usually used to investigate the energetically isolated system and the entropy S is the characteristic function. Based on the Boltzmann entropy $S = k_B \ln \Gamma_N(E)$ where $\Gamma_N(E)$ [7–9] is the number of microstates in a small energy interval $[E, E + \Delta E]$, the temperature is obtained from the thermodynamic relation $TdS = dE$. Although the analytical and numerical calculations of MC quantities have been used frequently for many years to study the properties of the finite systems [10–12], they rely on the arbitrary energy band ΔE. Therefore we adopt the Hertz entropy [13] within an energy sphere.

In recent years many works have shown that the MC thermodynamic functions exhibit nonanalytic behavior both in experiments [1,14,15] and in theory at the finite N classical [16–18] and quantum [19,20] systems. These nonanalyticities come from the inverted curvature entropy $S(E)$ with respect to E [20–22]; the origin is attributed to both the interaction [12,14,16,21,23] and the topology [24–26]. Apart from the nonanalyticities, some microscopic phase transitions have been predicted in classical small systems [14,21]. They originate from stationary points in energy functions [17,26,27]. However, the finite-size effects on the nonanalyticities of thermodynamic functions have not been given so far for finite noninteracting quantum gases. Note that such nonanalyticities occur for a perfectly smooth Hamiltonian, so they are not introduced artificially. Except for the interaction, stationary points of the energy function, and topology we expect that the trap geometries, boundary conditions, and energy spectrum configurations also dominate the nonanalyticities of thermodynamic functions for a thermally isolated system with a regulated energy injection. There still exist some open questions, such as how the nonanalytic thermodynamic functions can occur in small systems and how can these phenomena be interpreted even for the simplest ideal gas. In the MC ensemble, little is known about the analyticity properties of the MC entropy function even for the finite noninteracting gases. In this article, based on the exact recurrence relation for the MC partition function for finite and isolated noninteracting Bose gases in traps with different boundary conditions, we focus on the properties of the thermodynamic functions without the continuous spectrum approximation and thermodynamic limit. We find the presence of a series of inverted curvatures of the MC entropy function and the occurrence of the temperature and specific heat oscillations, including microscopic phase transitions and negative specific heats, when the energy spectrum has various configurations in d-dimensional confined spaces. These novel phenomena show quite different behaviors with various three-dimensional (3D) single-particle energy spectrum configurations when the systems are confined both in a rectangular box with the Dirichlet and periodic boundary conditions and in an anisotropic harmonic trap. We suggest that the entropy change (surface entropy) could be detected in the small system.

The paper is organized as follows. In Sec. II we briefly introduce the recurrence relation for the MC partition function

*ylma@fudan.edu.cn

and single-particle energy spectrum in different traps with various configurations, and derive the discrete thermodynamic quantities in the MC ensemble. In Sec. III we take the numerical analysis on the MC entropy, temperature, and specific heat of the finite noninteracting Bose gases; study their nonanalyticities due to the different trap geometries, boundary conditions, and energy spectrum configurations; and discuss the particle-number-dependent entropy change and critical temperature. Conclusions are made in Sec. IV.

II. EXACT PARTITION FUNCTIONS AND THERMODYNAMIC QUANTITIES

To study the thermodynamic properties of the finite system, we have to know the partition function first. Let Z_N and $\Gamma_N(E)$ be the canonical and MC partition functions with the independent system variables (N,T,V) and (N,E,V), respectively, one has

$$Z_N = \sum_E e^{-\beta E}\Gamma_N(E), \tag{1}$$

with inverse temperature $\beta = 1/(k_B T)$. There is a powerful recurrence relation for the canonical partition function [28–31]

$$Z_N = \frac{1}{N}\sum_{j=1}^{N}(\pm)^{j+1} z_j Z_{N-j}, \tag{2}$$

for the ideal bosonic (+) and fermionic (−) systems with $Z_0 = 1$, and $z_j = \sum_s \exp(-j\beta\varepsilon_s)$ being the single-particle partition function with the energy spectrum ε_s. Equation (2) appeared much earlier in the literature [32–34]. The recurrence formula of the exact MC partition function is [29]

$$\Gamma_N(E) = \frac{1}{N}\sum_{j=1}^{N}(\pm)^{j+1}\sum_s \Gamma_{N-j}(E - j\varepsilon_s), \tag{3}$$

with $\Gamma_0(x) = \delta_{0,x}$, where s stands for quantum numbers which labels a given single-particle state. There are many kinds of methods to derive this exact MC partition function, such as combinatorial techniques developed earlier in statistical nuclear fragmentation models [35] and a counting statistics method [28]. For the fixed N and E, all $\Gamma_{N-j}(E - j\varepsilon_s)(j = 1,2,\ldots,N)$ can be calculated within the conditions $\Gamma_0(0) = 1$ and $\Gamma_0(x \neq 0) = 0$. When we consider a boson system with a discrete spectrum $\varepsilon_s(s = 0,1,2,\ldots)$, it is important to point out that the total energy E must be some discrete value in keeping conservations of N and E. For example, $N = 1$, according to Eq. (3), one has $\Gamma_1(E) = \sum_s \Gamma_0(E - \varepsilon_s) = \delta_{E,\varepsilon_s}$. This means that the microstate number could equal 1 when the energy E is equal to a single-particle one. For $N = 2$, one has $\Gamma_2(E) = \frac{1}{2}\sum_s[\Gamma_1(E - \varepsilon_s) + \Gamma_0(E - 2\varepsilon_s)] = \frac{1}{2}\sum_{s,s'}\Gamma_0(E - \varepsilon_s - \varepsilon_{s'}) + \frac{1}{2}\sum_s \Gamma_0(E - 2\varepsilon_s)$. This implies that the two-particle system could be made up only by two particles in the same state and in different states. So we can calculate the microstate numbers with N particles through the recurrence relation Eq. (3) and the microstate number will be added when the energy $E = n_N\varepsilon_s$, with n_N being some integers.

The N-body system's energy is given by the Hamiltonian $H = \sum_{s=0}^{\infty}\varepsilon_s n_s$ with the occupation numbers being assumed values of $n_s = 0,1,2,\ldots$. The primary characteristic function of the MC ensemble is the Boltzmann shell entropy $S = k_B \ln\Gamma_N(E)$ [20,36–39], but there exists the arbitrary energy band ΔE within the energy sphere shell $E \leqslant H \leqslant E + \Delta E$. Even if, in the classical MC ensemble, this entropy function is inappropriate for systems in one-dimensional (1D) and two-dimensional (2D) spaces [18,36]. In the quantum MC ensemble with the box trapped potential, our calculated results show that this entropy is a high, frequently discontinuous function of the total energy E and the MC temperature will be negative at the small energy region. So the shell entropy is inapposite and a Hertz bulk entropy is reasonable (see the review in Ref. [13] for the employment of the bulk entropy). We need to adopt the partition function $\Omega_N(E)$ and the bulk entropy $S_N(E,V)$ within the sphere $0 \leqslant H \leqslant E$ as

$$\Omega_N(E) = \sum_{E_s=0}^{E}\Gamma_N(E_s), S_N = k_B \ln\Omega_N(E), \tag{4}$$

where E_s is all possible energy of the system. If S_N is a continue function of E, the temperature T, and specific heat C_N in the MC ensemble are obtained by [20,36–39]

$$\frac{1}{T} = \frac{\partial S_N}{\partial E}, \quad C_N = \left(\frac{\partial T}{\partial E}\right)^{-1} = -\frac{(\partial S_N/\partial E)^2}{\partial^2 S_N/\partial E^2}. \tag{5}$$

For the given physical system under consideration, all thermodynamical quantities are very sensitive to the energy spectrum ε_s.

We consider a noninteracting N-particle Bose gas system confined in a d-dimensional rectangular box with sides L_j and volume $V = L^d$. Here $d = 2,3$ will be considered below and $L = (\prod_{j=1}^{d} L_j)^{1/d}$ is the geometry average of the sizes. We have $L_j = \frac{L}{l_j}(\prod_{i=1}^{d} l_i)^{1/d}$ with any values of l_j for various geometry sizes of the trapping box, keeping the constant volume $V = L^d$. With Dirichlet boundary conditions (i.e., with impenetrable walls), the wave functions have to vanish at the walls of the container, and the single-particle spectrum is given by

$$\varepsilon_s^{(Dc)}(\{l_j\}) = \varepsilon_0^{(Dc)}\left(\prod_{i=1}^{d} l_i\right)^{-2/d}\sum_{j=1}^{d} l_j^2 s_j^2, \quad (s_j = 1,2,3,\ldots), \tag{6}$$

where $\varepsilon_0^{(Dc)} = \frac{\pi^2\hbar^2}{2mL^2}$ and the ground-sate energy is $3\varepsilon_0^{(Dc)}$. With periodic boundary conditions, the single-particle energy level is

$$\varepsilon_s^{(pc)}(\{l_j\}) = \varepsilon_0^{(pc)}\left(\prod_{i=1}^{d} l_i\right)^{-2/d}\sum_{j=1}^{d} l_j^2 s_j^2, \quad (s_j = 0, \pm 1, \pm 2, \pm 3, \ldots), \tag{7}$$

with $\varepsilon_0^{(pc)} = \frac{2\pi^2\hbar^2}{mL^2} = 4\varepsilon_0^{(Dc)}$ being the first excitation energy since the ground-state energy vanished. Although the single-particle spectra Eqs. (6) and (7) look very similar, the constant $\epsilon_0^{(Dc,pc)}$ and the allowed values of s_j are different. In the Dirichlet boundary condition, s_j cannot be zero, this will result in a great effect on the microstate numbers. In a d-dimensional anisotropic harmonic trapping potential,

$U(\{x_j\}) = \frac{1}{2}m\sum_{j=1}^{d}\omega_j^2 x_j^2$ with ω_j the trap frequency in the x_j direction. Let $\omega = (\prod_{j=1}^{d}\omega_j)^{1/d}$ be the geometry average of the trapping frequencies. From $\omega_l L_j = \text{constant}$ we have $V \propto \omega^{-d}$ and $\omega_j = \omega l_j(\prod_{i=1}^{d} l_i)^{-1/d}$. The single-particle energy spectrum reads

$$\varepsilon_s^{(ho)}(\{l_j\}) = \varepsilon_0^{(ho)}\left(\prod_{i=1}^{d} l_i\right)^{-1/d} \times \sum_{j=1}^{d} l_j\left(\frac{1}{2}+s_j\right), \quad (s_j = 0,1,2,\ldots), \quad (8)$$

with $\varepsilon_0^{(ho)} = \hbar\omega$.

As mentioned above, the MC total energy is discrete without both the continuous spectrum approximation and the thermodynamic limit in small systems. Due to the strong constraints of $N = \sum_{s=0}^{\infty} n_s$ and $E = \sum_{s=0}^{\infty} n_s\varepsilon_s$ in the MC ensemble, the system's total energy must be some discrete values like $E_n = n\varepsilon_0^{(Dc,pc,ho)}$ with n being the given integer, which have been included in the recursion formula (3). It is worth pointing out that the energy level numbers are infinite, but we only use finite energy levels to calculate entropy. Obviously the entropy is also a discontinuous function of the total energy, and we only get some discrete data of $S_N(E_n)$. Thus we have to calculate the thermodynamic functions using the difference instead of the differential

$$\frac{1}{T(E_{n+1})} = \frac{S_N(E_{n+1}) - S_N(E_n)}{E_{n+1} - E_n}, \qquad C_N = \frac{E_{n+1} - E_n}{T(E_{n+1}) - T(E_n)}. \quad (9)$$

Within the single-particle spectra Eqs. (6), (7), and (8) in the different traps, the single-particle energy can only be the multiple of $\varepsilon_0^{(Dc,pc,ho)}$. Since the system's total energy is also the multiple of $\varepsilon_0^{(Dc,pc,ho)}$, we can calculate the thermodynamic functions using the difference instead of the differential, and the least common multiple (difference interval) is just $\varepsilon_0^{(Dc,pc,ho)}$. Of course, every discrete point E_n is always the stationary point of the system energy.

III. NUMERICAL ANALYSIS OF THERMODYNAMICS

According to the exact recurrence formula Eqs. (3) and (4) of the MC partition functions, we now calculate the MC thermodynamic functions Eqs. (4) and (9). Because the total energy is discrete, the entropy functions are also discrete data in the MC ensemble. The calculated data are shown in Fig. 1 for $N = 30$ with all $l_j = 1$ for a simple cubic box and isotropic harmonic traps. Figures 1(a), 1(b), and 1(c) are for the simple cubic box trap with Dirichlet boundary conditions. In Fig. 1(a), the entropy function exhibits a series of convex and concave intruders [as magnified in Fig. 1(d) and explained below]. These intruders result in strong temperature fluctuations across the low-energy region [as shown in Fig. 1(b) and its magnification in Fig. 1(e)] and the specific heat oscillations [as shown in Fig. 1(c)], especially the negative values. The traditional smooth phase transition at e_c is shown in Fig. 1(f). Figures 2(a), 2(b), and 2(c) are for the simple

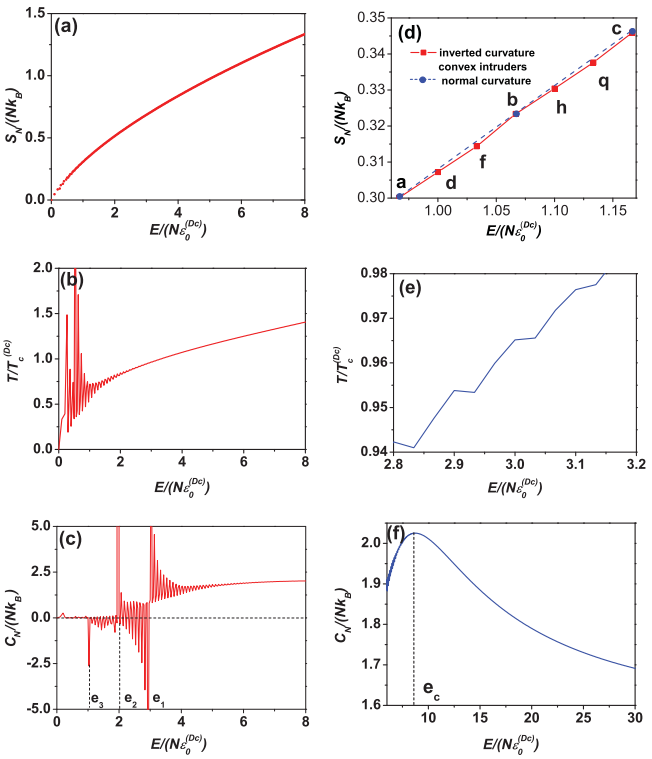

FIG. 1. (Color online) Three thermodynamic quantities vs. total energy per particle in units of $\varepsilon_0^{(Dc)}$ for $N = 30$ bosons confined in a simple cubic box trap with Dirichlet boundary conditions. (a) MC entropy S_N per particle in units of k_B. (b) MC temperature T in units of the noninteracting-gas thermodynamic transition temperature $T_c^{(Dc)}$. (c) MC specific heat C_N per particle in units of k_B. (d) The magnification of (a) showing the normal curvature (blue circle, dashed line) and the inverted curvature (red square, solid line). (e) The magnification of (b) showing the fluctuation of the caloric curve. (f) The magnification of (c) showing a smooth peak of the curve of C_N in the vicinity of $e_c = E_c/(N\varepsilon_0^{(Dc)})$.

cubic box trap with periodic boundary conditions (dashed blue lines) and for the isotropic harmonic trap (solid red lines). The nonanalyticities do not occur in this case due to the isotropic traps. They only have the smooth caloric temperature curves in Fig. 2(b) and smooth phase transitions at $e_c^{(pc,ho)}$ in Fig. 2(c). Here the 3D noninteracting-gas thermodynamic transition temperatures are $T_c^{(Dc,pc)} = 2\pi\hbar^2[N/V\zeta(3/2)]^{2/3}/mk_B$ and $T_c^{(ho)} = \hbar\omega[N/\zeta(3)]^{1/3}/k_B$ with $\zeta(\nu)$ the Riemann zeta function.

From Figs. 1 and 2 we can see, in the MC ensemble, the results for the simple cubic box trap with Dirichlet boundary conditions are totally different from the ones both for the simple cubic box trap with periodic boundary conditions and for the isotropic harmonic trap, the temperature is no longer increasing monotonously along with the energy [see Fig. 1(b)], and there exist nonanalytic behaviors, microscopic phase transitions, and negative specific heats [see Fig. 1(c)], some of which have been found both in the experiments and in other MC systems [14,15,18]. What is the most interesting are the fluctuations of T and C_N, in which the oscillations of temperature are generic and shared by all physical systems that are exhibited in the MC ensemble, and resulting in the

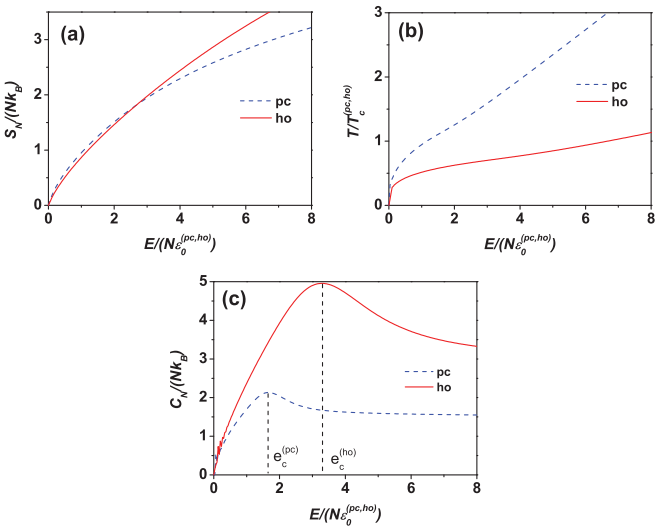

FIG. 2. (Color online) Three thermodynamic quantities vs. total energy per particle in units of $\varepsilon_0^{(pc,ho)}$ for $N = 30$ bosons confined in a simple cubic box trap with periodic boundary conditions (dashed blue lines) and a harmonic trap (solid red lines). (a) MC entropy S per particle in units of k_B. (b) MC temperature T in units of the noninteracting-gas thermodynamic transition temperatures $T_c^{(pc,ho)}$. (c) MC specific heat C_N per particle in units of k_B.

named microscopic phase transitions at e_1, e_2, and e_3. Mathematically, the microscopic phase transitions arise whenever the entropy grows nonsmoothly in the vicinity of some energy values.

Both in the simple cubic box trap with periodic boundary conditions and in the isotropic harmonic trap, the single-particle levels are $\varepsilon_\nu^{(pc,ho)} = \nu\varepsilon_0^{(pc,ho)}$ with ν being integers. So the total energy of the system with N particles is $E_n = n\varepsilon_0^{(pc,ho)}$ with n also being integers. Because of the uniformity of the single-particle levels, the amount of the states increases exponentially with the increase of the total energy. Therefore the curve of the entropy S_N is smooth in a concave curvature. But in the simple cubic box trap with the Dirichlet boundary conditions, the single-particle levels are $\varepsilon_\nu^{(Dc)} = \nu\varepsilon_{gs}^{(Dc)}$ with $\varepsilon_{gs}^{(Dc)} = 3\varepsilon_0^{(Dc)}$ being the ground-state energy. We know that ν are either integers like 1,2,3,4,6,..., or some fractions like $\frac{11}{3}, \frac{14}{3}, \frac{17}{3}, \ldots$. So the system's total energy is $E_n = n_f\varepsilon_{gs}^{(Dc)}$ with n_f either being integers or being a third of the integers. In the latter case, the single-particle levels are not uniform. Consequently, the number of levels with fraction ν is smaller than those with integer ν, and the amounts of the microstates with total energy of fraction n_f are smaller than those with the integer n_f. The entropies of the corresponding microstates are smaller accordingly, which we can see in Fig. 1(d) (the blue circles a, b, and c with integers n_f representing the normal S_N values while the red squares d, f, h, and q with fractions n_f have smaller S_N values than the normal values at the corresponding E_n). In Fig. 1(d), the (blue) dotted line (i.e., line segment abc) is a concave curve, like the curves in Fig. 2(a) generally, thus the specific heats are always positive if we use difference intervals between ab and bc. But the (red) solid line consists of two real convex curves (i.e., the line segments adfb and bhqc) and they are convex curves, while the line segment fbh is also a concave curve. The tiny entropy difference results in the curve being convex and concave in the different regions. So the specific heats are positive and negative alternately, which is shown in Fig. 1(c). When increasing S_N a little at the red square for decreasing S_N a little at the blue circle b, the caloric curve will become flat in this energy region [as shown in Fig. 1(b)]. This leads to infinite negative and positive specific heats in different regimes, which means the microscopic phase transitions occur in positions of energies e_1, e_2, and e_3, as shown in Fig. 1(c). Every nonanalyticity point at E_n is always the stationary point of the system energy.

The nonanalytic behaviors are important and basic characteristics of the finite noninteracting Bose gases. To study the properties of the nonanalyticities, we consider the 3D box traps in different geometry sizes with different energy level configurations under the Dirichlet boundary conditions. For simplification, we take $l_1 = 1$, $l_2^2 = l$, and $l_3^2 = \frac{1}{l}$ with a single geometry parameter l. Figure 3 shows the specific heat curves for $N = 30$ with $l = 2,3,\ldots,7$. In Figs. 3(a), 3(b), and 3(e) for $l = 2$, 3, and 6, the numbers of peaks are two, three, and four, respectively, but Figs. 3(c), 3(d), and 3(f) for $l = 4$, 5, and 7 show the complicated behaviors (i.e., there exist many oscillations and microscopic phase transitions). Besides the number of peaks, the heights and positions of the peaks are also different with different configurations. Some peaks have infinite positive and finite negative values while other peaks have finite positive and infinite negative values. Generally speaking, the heights of the peaks increase with increasing system energy.

For the noninteracting Bose gases, the microscopic oscillations of MC thermodynamic quantities occur in special kinds of energy level configurations that are determined only by the geometry property of the system. The different traps with different boundary conditions result in different energy level configurations. So the boundary types and conditions are a key point. Generally, it is natural to expect that if there is no boundary, there is no boundary effect at all. But even in the periodic boundary conditions, the structures of a discrete spectrum with various energy level configurations still have an effect on the properties of the finite system. Figure 4 shows the specific heat curves of different geometry parameters for the 3D box traps with periodic boundary conditions. For $(l_1^2, l_2^2, l_3^2) = (1,1,2)$, Fig. 4(a) still does not show any oscillations except for at very low energy. Of course, it only shows a smooth phase transition like in Fig. 2(c). For other geometry parameters, Figs. 4(b), 4(c), and 4(d) show the complicated oscillation behaviors in small energy regions. Figures 4(b) and 4(d) with similar behaviors show the nonanalyticities and microscopic phase transitions, especially the infinite negative specific heats, and Fig. 4(c) is similar to Figs. 3(c), 3(d), and 3(f).

We all know that there do not exist any phase transitions for the 2D Bose system in the thermodynamic limit. But in small 2D Bose systems with finite particles and different boundary conditions, the results are indeed not the same with those in the thermodynamic limit. Figure 5 are our calculated results on the specific heats for $N = 30$ bosons trapped in a 2D box of different sizes with different boundary conditions. Figure 5(a) is the C_N curve in the square box trap under the Dirichlet

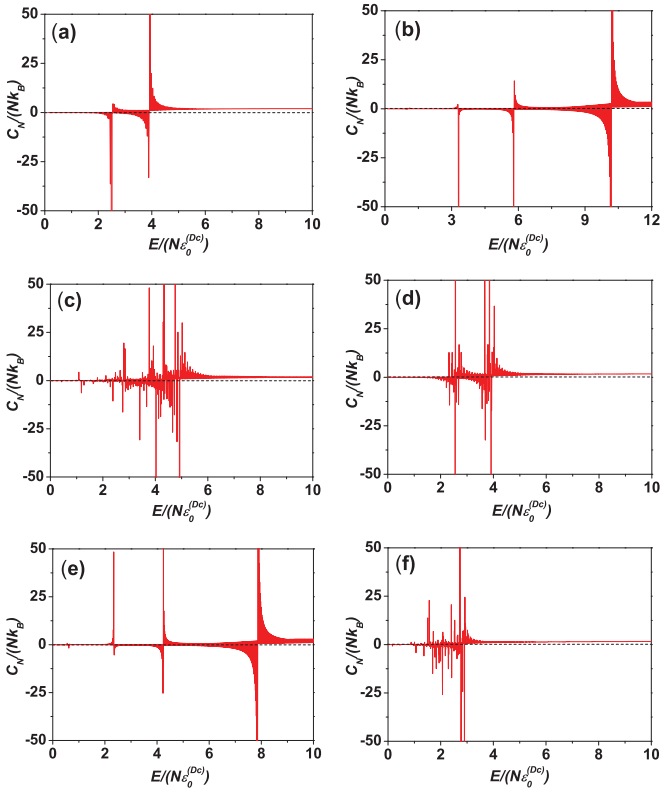

FIG. 3. (Color online) MC specific heat C_N per particle in the units of k_B vs. total energy per particle in units of $\varepsilon_0^{(Dc)}$ for $N = 30$ bosons confined in a rectangular box trap under Dirichlet boundary conditions with different geometry parameters $(1,l,1/l)$: (a) $l = 2$, (b) $l = 3$, (c) $l = 4$, (d) $l = 5$, (e) $l = 6$, and (f) $l = 7$.

boundary conditions. It shows that there also exist many small oscillations, three microscopic phase transitions, and a small smooth peak of C_N at e_c (see the inset). This is similar to the 3D Bose systems. The small peak indicates that there exists a smooth phase transition in 2D small systems. Figure 5(b) is the C_N curve in the square box trap under the periodic boundary conditions. Although there exists a small smooth peak in the low-energy region, it is not like the peak in Fig. 5(a). This is because the small smooth peak will vanish when particle numbers go to infinity. Of course, there exist C_N fluctuations in the low-energy region, but not negative specific heats. The high-energy behaviors are also different with the different boundary conditions [see the insets of Figs. 5(a) and 5(b)]. Figures 5(c) and 5(d) show clearly the oscillations of the specific heats (including the microscopic phase transitions and negative specific heats) with the 2D rectangular box of sides $(2^{1/4},2^{-1/4})L$ and $[(5/4)^{1/4},(4/5)^{1/4}]L$ under the Dirichlet and periodic boundary conditions, respectively. Obviously, from Figs. 3(c), 3(d), 3(f), 4(b), 4(c), 4(d), and 5(d) we can see that the complicated oscillation behaviors occur at the relative small-energy regions.

We also know that all the curves tend to be the thermodynamic limit when N goes to infinity. Figure 6(a) shows the entropy S_N as a function of N in the MC ensemble in the simple cubic box trap with the Dirichlet (solid red line) and periodic (dashed blue line) boundary conditions. Here we take the total energy per particle $\frac{E}{N} = f\frac{\pi^2\hbar^2}{2m}(\frac{N}{V})^{2/3}$ as a constant at a normal

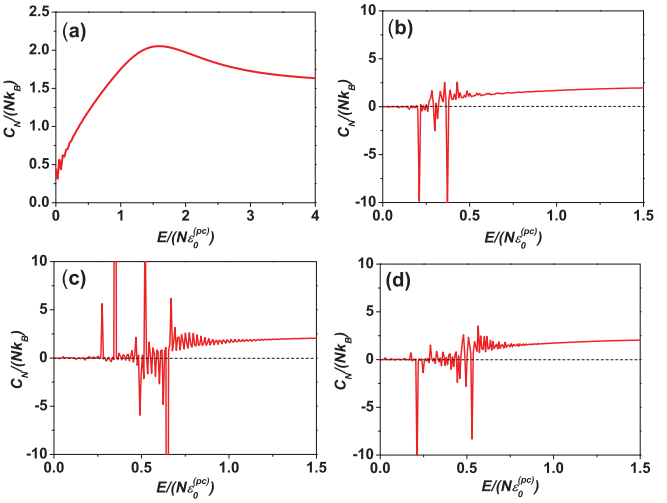

FIG. 4. (Color online) MC specific heat C_N per particle in units of k_B vs. total energy per particle in units of $\varepsilon_0^{(pc)}$ for $N = 30$ bosons confined in a rectangular box trap with periodic boundary conditions. Geometry parameters (l_1^2,l_2^2,l_3^2) are chosen as (a) (1,1,2), (b) (2,5,7), (c) (3,5,6), and (d) (3,5,7).

state when the particle density N/V keeps constant with $f = 1(4)$ under the Dirichlet (periodic) boundary conditions. When $N \gg 1$ the entropy approaches the thermodynamic limit of $s_\infty = 5\mathrm{Li}_{5/2}(z)/2\mathrm{Li}_{3/2}(z) - \ln z = 3.665Nk_B$ [see the dotted gray line in Fig. 6(a)]. Here the fugacity $z = 0.2726$ is the solution of the equation $3\mathrm{Li}_{5/2}(z) = 2\pi\mathrm{Li}_{3/2}^{5/3}(z)$ at fixed E/N and $T/T_c^{(Dc,pc)} = [\mathrm{Li}_{3/2}(1)/\mathrm{Li}_{3/2}(z)]^{2/3} = 4.199$ with $\mathrm{Li}_\nu(z)$ being the polylogarithm function. In the thermodynamic limit, the entropy per particle $s_\infty = S_N/Nk_B$ is a macroscopic extensive control parameter for N and V going to infinity, but keeping N/V to a constant. However, in the finite

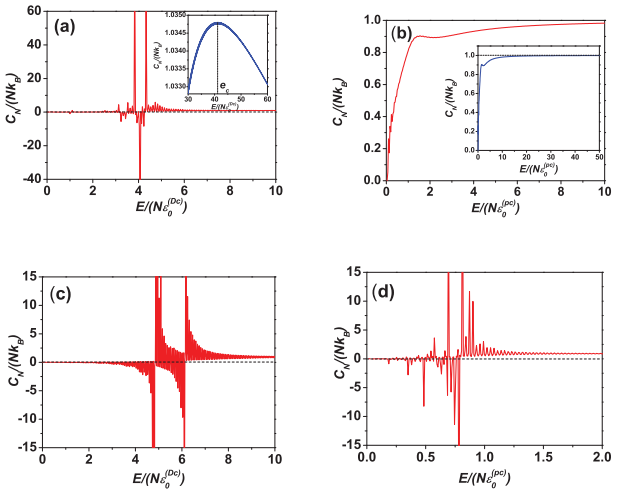

FIG. 5. (Color online) MC specific heat C_N per particle in the units of k_B vs. total energy per particle in the units of $\varepsilon_0^{(Dc,pc)}$ for $N = 30$ bosons confined in a two dimensional box trap with the Dirichlet [(a) and (c)] and periodic [(b) and (d)] boundary conditions. Geometry parameters (l_1^2,l_2^2) are chosen as (a) (1,1), (b) (1,1), (c) (1,2), and (d) (4,5).

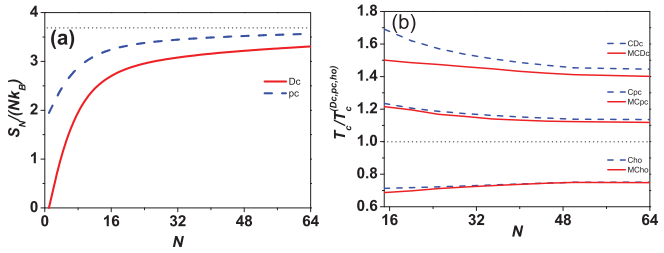

FIG. 6. (Color online) (a). Entropy S_N per particle in units of k_B vs. particle number N in the MC ensemble in the simple cubic box trap with the Dirichlet (solid red line) and periodic (dashed blue line) boundary conditions. (b). The transition temperature $T_c(N)$ in units of the 3D noninteracting-gas thermodynamic transition temperatures $T_c^{(Dc,pc)} = 2\pi\hbar^2[N/V\zeta(3/2)]^{2/3}/mk_B$ and $T_c^{(ho)} = \hbar\omega[N/\zeta(3)]^{1/3}/k_B$ vs. particle number N in the MC and canonical ensembles in the simple cubic boxes with the Dirichlet and periodic boundary conditions and in the isotropic harmonic trap. Solid red lines of MCDc, MCpc, and MCho present in the MC ensemble and dashed blue lines of CDc, Cpc, and Cho present in the canonical ensemble with the Dirichlet and periodic boundary conditions and in the harmonic trap, respectively.

system, the entropy S_N is a naturally nonextensive quantity and entropy per particle s_N includes the interesting finite-size information. The entropy change $s_N - s_\infty$ presents the surface entropy due to the boundary effects. We can see in Fig. 6(a) that the surface entropy increases with the decrease of N. This entropy change should be observable in suitably designed experiments for fixed E/N and N/V of the finite systems.

Finally, having obtained the canonical partition function Eq. (2) with the corresponding spectra for the systems under consideration, we can determine the canonical specific heat according to $C_N = k_B T \frac{\partial^2}{\partial T^2}(T \ln Z_N)$. We define the maximum specific heat corresponding temperature as the canonical transition temperature. We have compared the transition temperatures in the different ensembles with different traps and boundary conditions. The results have been shown in Fig. 6(b). We can see that the transition temperatures in the canonical ensemble are a little higher than the ones in the MC ensemble, and the difference is larger with the Dirichlet boundary conditions. With increasing N, the transition temperatures with the Dirichlet boundary conditions in the canonical ensemble decrease faster than those in the MC ensemble. These indicate the nonequivalence between the two ensembles, especially in the finite systems with different physical boundaries. When particle number N increases to infinity the transition temperatures approach the ones of the thermodynamic limits $T_c^{(Dc,pc)}$ and $T_c^{(ho)} = \hbar\omega[N/\zeta(3)]^{1/3}/k_B$ [see the dotted gray line in Fig. 6(b)].

IV. CONCLUSION

We have investigated the nonanalyticities of the MC thermodynamic functions in the small noninteracting Bose systems confined both in the d-dimensional rectangular boxes with the Dirichlet and periodic boundary conditions and in the d-dimensional anisotropic harmonic traps. We have shown that there exist the nonmonotonous temperature dependence on E, nonanalytic and negative specific heats, and microscopic phase transitions. These novel behaviors are due to the finite trap-size effects and come from a series of inverted curvature concave intruders in the bulk entropy function $S_N(E)$ for fixed N and V. Their microscopic origin is the various single-particle energy spectrum configurations with different trap types and sizes, which is related to the configuration space topology and the stationary point in the energy function. It is not a surprise that there exist BEC in the 2D small ideal Bose system which could not occur in the thermodynamical limit. The behaviors of the $T_c(N)$ curve have obvious differences between the MC and canonical ensembles for small systems. Almost all the results of the thermodynamical quantities approach the thermodynamical limit for large enough N.

For the finite noninteracting Bose gases trapped in different potentials with different boundary conditions, we do not take the continuous spectrum approximation and this is not the thermodynamic limit. The discrete entropy per particle $s_N = S_N(E,V;\{l_j\})/Nk_B$ as a function of MC variables (N,E,V) and various energy spectrum configurations $\{l_j\}$ in the d-dimensional spaces has included all information of the thermodynamical properties. We emphasize the finite-size effects on the MC entropy change, which should, in principle, be observable in suitably designed experiments of the finite systems for fixed E/N and N/V. In the experiments with small particle numbers, very low densities, and finite volume, we should be able to detect the oscillating behaviors both in temperature and in specific heats like in the interacting system. To generalize this approach to interacting gas is of further interest. For the small systems with finite energy levels, novel and rich phenomena will occur. This is a work in progress and will be published elsewhere.

ACKNOWLEDGMENTS

This work was supported by the National Natural Science Foundation of China under Grants No. 10775032 and No. 10974033, and the Ministry of Education of China (Project No. B06011).

[1] M. Schmidt, R. Kusche, T. Hippler, J. Donges, W. Kronmüller, B. von Issendorff, and H. Haberland, Phys. Rev. Lett. **86**, 1191 (2001).

[2] M. Schmidt, T. Hippler, J. Donges, W. Kronmüller, B. von Issendorff, H. Haberland, and P. Labastie, Phys. Rev. Lett. **87**, 203402 (2001).

[3] M. Klindworth, A. Melzer, A. Piel, and V. A. Schweigert, Phys. Rev. B **61**, 8404 (2000).

[4] A. Melzer, M. Klindworth, and A. Piel, Phys. Rev. Lett. **87**, 115002 (2001).

[5] C. Bréchignac, Ph. Cahuzac, B. Concina, and J. Leygnier, Phys. Rev. Lett. **92**, 083401 (2004).

[6] C. J. Pethick and H. Smith, *Bose-Einstein Condensation in Dilute Gases* (Cambridge University Press, Cambridge, England, 2002); L. Pitaevskii and S. Stringari, *Bose-Einstein Condensates* (Clarendon Press, Oxford, 2003).
[7] L. D. Landau and E. M. Lifshitz, *Statistical Physics* (Pergamon, Oxford, 1980).
[8] K. Huang, *Statistical Mechanics*, 2nd ed. (Wiley, New York, 1987).
[9] C. Kittel, *Elementary Statistical Physics* (Wiley, New York, 1958).
[10] J. Lee and J. M. Kosterlitz, Phys. Rev. Lett. **65**, 137 (1990).
[11] P. Labastie and R. L. Whetten, Phys. Rev. Lett. **65**, 1567 (1990).
[12] D. H. E. Gross and J. F. Kenney, J. Chem. Phys. **122**, 224111 (2005).
[13] M. Campisi, e-print arXiv:0709.1082v1.
[14] C. Junghans, M. Bachmann, and W. Janke, Phys. Rev. Lett. **97**, 218103 (2006).
[15] F. Gobet, B. Farizon, M. Farizon, M. J. Gaillard, J. P. Buchet, M. Carré, P. Scheier, and T. D. Märk, Phys. Rev. Lett. **89**, 183403 (2002).
[16] S. Hilbert and J. Dunkel, Phys. Rev. E **74**, 011120 (2006).
[17] M. Kastner and O. Schnetz, J. Stat. Phys. **122**, 1195 (2006).
[18] J. Dunkel and S. Hilbert, Physica A **370**, 390 (2006).
[19] D. C. Brody, D. W. Hook, and L. P. Hugston, Proc. R. Soc. London A **463**, 2021 (2007).
[20] D. H. E. Gross, *Microcanonical Thermodynamics* (World Scientific, Singapore, 2001).
[21] D. H. E. Gross, A. Ecker, and X. Z. Zhang, Ann. Physik **5**, 446 (1996).
[22] W. Janke, Nucl. Phys. B, Proc. Suppl. **63A-C**, 631 (1998).
[23] L. Casetti and M. Kastner, Phys. Rev. Lett. **97**, 100602 (2006).
[24] M. Kastner, Rev. Mod. Phys. **80**, 167 (2008).
[25] M. Kastner, Physica A **359**, 447 (2006).
[26] L. Casetti, M. Kastner, and R. Nerattini, J. Stat. Mech. (2009) P07036.
[27] M. Kastner, e-print arXiv:1010.4437v1.
[28] M. Wilkens and C. Weiss, J. Mod. Opt. **44**, 1801 (1997); C. Weiss and M. Wilkens, Opt. Express **1**, 272 (1997).
[29] P. Borrmann, J. Harting, O. Mülken, and E. R. Hilf, Phys. Rev. A **60**, 1519 (1999).
[30] K. Glaum, H. Kleinert, and A. Pelster, Phys. Rev. A **76**, 063604 (2007).
[31] J. H. Wang and Y. L. Ma, Phys. Rev. A **79**, 033604 (2009).
[32] P. T. Landsberg, *Thermodynamics* (Interscience, New York, 1961).
[33] H. Schmidt, Am. J. Phys. **57**, 1150 (1989).
[34] P. Borrmann and G. Franke, J. Chem. Phys. **98**, 2484 (1993).
[35] K. C. Chase, A. Z. Mekjian, and L. Zamick, e-print arXiv:cond–mat/9708070 v1 (1997).
[36] R. Becker, *Theory of Heat* (Springer, New York, 1967).
[37] A. Münster, *Statistical Thermodynamics* (Springer, Berlin, 1969).
[38] E. M. Pearson, T. Halicioglu, and W. A. Tiller, Phys. Rev. A **32**, 3030 (1985).
[39] T. Cagin and J. R. Ray, Phys. Rev. A **37**, 247 (1988).